X-716-65-410

NASA TM X-55385

PRELIMINARY RESULTS OF THE EXPLORER XXVI SOLAR CELL EXPERIMENT

OCTOBER 1965

NASA

GODDARD SPACE FLIGHT CENTER

GREENBELT, MARYLAND

X-716-65-410

PRELIMINARY RESULTS OF THE EXPLORER XXVI SOLAR CELL EXPERIMENT

by

Luther W. Slifer, Jr.
and
Stephen G. McCarron

October 1965

PRELIMINARY RESULTS OF THE EXPLORER XXVI SOLAR CELL EXPERIMENT

ABSTRACT

To determine the integrated radiation effects on solar cells in an intense radiation orbit, an experiment consisting of four, 10-cell, series strings of N/P solar cells was mounted on one of the body facets of the Explorer XXVI spacecraft. Two strings were composed of 1 ohm-cm cells and two of 10 ohm-cm cells. One string of each base resistivity had a 6-mil glass shield and the other of each base resistivity had a 60-mil glass shield. A precision resistor across each string loaded it near the peak power point. The voltage drop across this load was measured and converted to current. The current was normalized on the basis of pre-launch calibrations for angle of incidence and comparisons were made. Preliminary results of this engineering experiment are presented. They show that, in this orbit, the 10 ohm-cm cells with a 6-mil shield provided significantly better radiation resistance than 1 ohm-cm cells with the same glass. When the heavy shield (60-mil glass) is used, the increased resistance is equally significant. The results also show that the use of the higher base resistivity cell provides a significant fraction of the radiation protection afforded by the heavy 60-mil cover glasses but at no cost in weight.

CONTENTS

	Page
ABSTRACT	iii
LIST OF TABLES	vi
LIST OF ILLUSTRATIONS	vi
INTRODUCTION	1
THE EXPERIMENT	1
Purpose	1
Approach	1
CALIBRATION AND DATA REDUCTION	3
Satellite Rotation Effects	3
Sunline-Spin Axis Angle Effects	3
Solar Constant Effects	4
Normalization of Current and Power	4
RESULTS	5
Spacecraft	5
Solar Panel	6
ANALYSIS AND DISCUSSION	6
1 Ohm-cm Cells, 6 Mil Shields	7
10 Ohm-cm Cells, 6 Mil Shields	8
1 Ohm-cm Cells, 60 Mil Shields	9
10 Ohm-cm Cells, 60 Mil Shields	9
Constant Voltage Operation	9
Selected Orbits	10
Correlation with Laboratory Measurements	11
Equivalent Flux	11
CONCLUSIONS AND RECOMMENDATIONS	12
ACKNOWLEDGMENTS	13
REFERENCES	13

LIST OF ILLUSTRATIONS

Figure		Page
1	The Explorer XXVI Satellite During Spin Tests	15
2	The Explorer XXVI Solar Cell Experiment Panel	16
3	Aspect Calibration for the Various Experiment Cell Strings	17
4	Solar Constant Correction Factor	18
5	Aspect Variation During the Time Period Studied	19
6	Experiment Panel Temperature Variation During the Time Period Studied	20
7	Solar Cell Voltage Variation During the Time Period Studied	21
8	Normalized Current Degradation During the Time Period Studied	22
9	Normalized Power Degradation During the Time Period Studied	23
10	Sketch Depicting the Effect of the Load Point on the Degradation Readings	24

LIST OF TABLES

Table		Page
I	Solar Cell Experiment	2
II	Launch and Orbit Parameters for Explorer XXVI	5
III	Degradation Results for Selected Orbits	10
IV	Nominal Equivalent Flux Values for the Various Cell Conditions	11

PRELIMINARY RESULTS OF THE EXPLORER XXVI SOLAR CELL EXPERIMENT

INTRODUCTION

In 1962, after the effects of the Starfish high-altitude nuclear explosion resulted in a review of the radiation resistance of solar cells, it was determined that conversion from P/N solar cells to N/P solar cells was required. Extensive radiation damage comparison tests were performed at the Naval Research Laboratory on N/P cells from various American manufacturers to determine the status and relative merits of their production capabilities [1, 2]. In addition, these same cells were tested to obtain detailed information on their performance characteristics [3]. In May 1963 preparation of a follow-on to the SERB satellite was begun, presenting the opportunity to obtain flight information on cells from these same production lots. Authorization to fly such a solar cell experiment on a non-interference basis was requested and received.

THE EXPERIMENT

Purpose

Results of prior testing of N/P solar cells had shown that, in laboratory experiments, cells with higher base resistivity exhibited a better radiation resistance than cells with lower base resistivity [1, 2, 4]. On the basis of these results most cell manufacturers were developing a capability for producing cells with higher base resistivities. The primary purpose of the solar cell experiment was to substantiate (or refute) the validity of the generalization of the results of monoenergetic electron and proton tests to the space radiation environment where an inhomogeneous flux is experienced. (A secondary purpose of the experiment was to provide a comparison of the performance of N/P solar cells to the P/N cells in the spacecraft power supply but will not be discussed here.)

Approach

In order to accomplish these objectives the experiment was designed as shown in Table I. Two rows of cells were provided for each of the two base resistivities — 1 ohm-cm and 10 ohm-cm. One row of each base resistivity type had a 6 mil coverglass and the other of each type had a 60 mil coverglass. In the space environment the 6 mil glasses would stop only the low energy protons (below 4.5 Mev) subjecting the cells to all other radiation while the 60 mil

Table I

SOLAR CELL EXPERIMENT

Cell Strings		Solar Cells				Cover Glasses		
Row No.	Symbol (See Fig.)	No. in Series	Type	Mfg (Ref 1,2)	Nom Base Resistivity (ohm-cm)	Type (Corning)	Thick-ness (mil)	Load Resistor (ohms)
1	⊙	10	N/P	C	1	0211	6	100
2	●	10	N/P	C	1	7940	60	100
3	■	10	N/P	F	10	7940	60	90
4	⊡	10	N/P	F	10	0211	6	90

glasses would stop protons with energies below 17 Mev and attenuate electron energies thus limiting damage to that produced by high energy particles. In this way it was intended that comparisons could be made of differences in radiation resistance to the two general categories of irradiation. (The use of the 60 mil shields also provided for comparisons with the spacecraft power supply which used 60 mil shields.)

Previously fixed mechanical and electrical interface requirements precluded optimization of the experiment. The number of cells used in series was limited (by the panel area) to ten, the choice of load resistors was restricted by the desire for a sizable signal in a 0-5 volt telemetry output range, and location of the experiment on one of the body facets made it sensitive to variations in both the aspect and the rotation of the satellite. The spinning satellite is shown in Figure 1.

As a result of the above restrictions, the precision load resistors, used across each cell string, were chosen so as to load the cells in the vicinity of the peak power point. In addition, some degree of matching of the initial space outputs for the various rows of cells was accomplished. A 100 ohm resistor was used for the 1 ohm-cm cells and a 90 ohm resistor was used for the 10 ohm-cm cells.

The temperature was monitored by the use of a calibrated thermistor imbedded in the panel. It was located near the geometrical center of the panel just below the aluminum skin on which the cells were mounted.

In order to assure a stable assembly of the solar cell experiment, radiation effects on various adhesives were studied and two pre-prototype panels were subjected to environmental tests[5]. Results of these tests led to the choice of a flat-mounted cell assembly with silver expanded-metal interconnectors. RTV-40 (General Electric) was chosen to bond the cells to an aluminum skinned honeycomb substrate and Sylgard 182 (Dow Corning) was chosen as a coverglass adhesive. The completed solar cell experiment panel is shown in Figure 2.

CALIBRATION AND DATA REDUCTION

Since the illumination of the solar cells is dependent upon both the angle of incidence and the solar constant, correction for these effects is necessary in the process of data reduction.

Satellite Rotation Effects

The effect of satellite rotation was eliminated with the aid of a computer program which sorted and reduced the data. By correlating data from the optical aspect sensor with telemetry rates and times it was possible to determine angle of rotation of the satellite for each solar cell experiment data point. Data considered here are for satellite rotation angles of $180° \pm 2°$ measured from the aspect sensor. This is the rotational position at which the experiment panel faces the sun with variations from normal incidence being strictly sunline-spin axis angle variations.

Sunline-Spin Axis Angle Effects

The corrections for sunline-spin axis angle were accomplished using a pre-launch calibration of the experiment. This calibration was performed in sunlight on a clear (cloudless and haze-free to the naked eye) day using a collimator with a 10:1 length to aperture width ratio. The current variation with aspect angle was determined at a voltage of 50 mv/cell (or 500 mv for the 10-cell string) giving essentially the short circuit current variation. Deviations of the results from the cosine law are plotted in Figure 3 using the equation:

$$F(\psi) = \frac{I/I_{90}}{\text{Sin } \psi} \qquad (1)$$

where,

ψ is the sunline to spin axis (aspect) angle,
$F(\psi)$ is the aspect correction factor for this angle,
I is the current measured at this angle,

and

I_{90} is the current at normal incidence.

Note that, in this equation, $\sin \psi$ is used in applying the cosine law because the spin axis is perpendicular to the normal to the experiment. That is, the angle of incidence is $90°-\psi$.

It can be seen in Figure 3 that deviations from the cosine law were significant, going as high as 7%, for the 60 mil shields but relatively insignificant, generally less than 1%, for the 6 mil shields in the aspect range from 45° to 120° which proved to be the range of interest. Comparison of these curves also shows quite clearly that the deviations are primarily dependent on the coverglasses.

Solar Constant Effects

The variation of the solar constant is a result of the ellipticity of the earth's orbit and therefore a function of the day of the year. The correction factor, f(D), for this variation is plotted in Figure 4 [6].

Normalization of Current and Power

The above calibration and correction factors provided for normalization of the data to 140 mw/cm^2 insolance at normal incidence according to the equations:

$$I_N = \frac{I}{f(D)\, F(\psi)\, \sin \psi} \tag{2}$$

and,

$$P_N = I_N V \tag{3}$$

where,

I_N is the normalized current
P_N is the normalized power

and,

V is the voltage reading on the cell string.

I, V, and the precision load resistance, R, are interrelated by Ohm's Law.

RESULTS

Spacecraft

Launch and orbit data for the Explorer XXVI spacecraft are listed in Table II. The results considered here are for the first 540 orbits covering a time period of 171 days — the conversion factor being 3.16 orbits/day.

Table II

LAUNCH AND ORBIT PARAMETERS FOR EXPLORER XXVI

Launch Date	12/21/64
Perigee	309 km
Apogee	26,200 km
Inclination	20 degrees
Period	7.6 hours

Variation of the sunline-spin axis angle for this time period is shown in Figure 5[7]. Both at the beginning and at the end of this time period there is some question as to the exact aspect angle. This results from the fact that the aspect sensor reads in discrete steps and the only accurately known points are those where the readout changes from one step to the next. Thus, when there is no change, the angle can be determined only to an accuracy within the width of the step. This is indicated by the blocks in the figure. The extrapolation for the early portion of the curve was inferred from the panel temperature and the solar array current profile measurements and that for the later portion is a best estimate including the consideration that the aspect angle is reversing direction.

This figure indicates that the aspect angle started at about 47° and held fairly constant for a period of roughly 16 days or 50 orbits at which time it began to change, increasing to 90° (normal incidence) at 98 days or 310 orbits. It continued to an extreme of approximately 117° at about 171 days or 540 orbits.

Solar Panel

The experiment panel temperatures are plotted in Figure 6. These are temperatures averaged on an orbit basis but excluding the eclipsed portion of the orbit. Several features in the temperature-time history require discussion. First, it can be seen in the figure that two orbits were required for the panel to reach an equilibrium temperature after launch. This initial equilibrium temperature was then maintained essentially constant for the first 40 or 50 orbits indicating that the aspect angle was essentially constant. Secondly, because of the aspect variation, symmetry would ordinarily be expected about the 310 orbit (90° aspect) point. However, paddle shadowing during portions of the satellite rotation plus other, more complex contributing factors destroy this symmetry. Finally, the total variation in panel temperature was from 9°C to 20°C indicating that effects of temperature variations on the solar cells would be secondary in nature.

Voltage readings for the various cell rows on the solar panel are shown in Figure 7. These data points each represent average voltage values for an orbit excluding the portion when the satellite was eclipsed. Because the solar cells were loaded in the vicinity of the peak power point, these voltages are important as indicators of cell operating conditions and must be considered in the analysis and interpretation of the final results.

The voltage data were reduced as previously described and the resulting normalized current and power data are plotted in Figures 8 and 9 respectively in terms of percent of initial normalized values. Apparent anomalies in the data result from the "wandering" operating voltage and will be discussed later. A degradation grid for 1 Mev electron bombardment of bare 1 ohm-cm cells[8] is also plotted in these figures for reference. It should be noted that the grids are not necessarily accurate at low flux or degradation levels because of general measurement difficulties.

ANALYSIS AND DISCUSSION

The results depicted in Figures 8 and 9 appear confusing at first glance. Nevertheless, it is immediately clear that the 10 ohm-cm cells are significantly more radiation resistant than the 1 ohm-cm cells over the wide range of operating conditions experienced. Thus, the major objective of the experiment, that of determining whether laboratory test results showing 10 ohm-cm cells to be more radiation resistant than 1 ohm-cm cells could be generalized to space flight, was satisfied.

Closer analysis of the results (Figures 5 through 9) with reference to current-voltage curves as a function of radiation degradation[1] provides clarifying information. Operation for each of the cell strings is discussed qualitatively below in order to afford an understanding of the meaning and validity of the results shown in Figures 8 and 9. This is done in conjunction with the sketch in Figure 10 which depicts I-V curves for various cell conditions along with resistive load lines with differing relationships to the curves. This figure clearly illustrates that the current degradation ΔI is highly dependent on the operating point — the significant factor in the following discussion.

1 Ohm-cm Cells, 6 Mil Shields

Since the initial operating voltage for these cells was 399 mv/cell, a load similar to R_1 as related to curve (a) is indicated. During the first 40 orbits the voltage dropped to 345 mv/cell. Since the angle of incidence and the temperature both remained constant during this time, the voltage variation can be considered almost entirely the result of radiation degradation. That is, the I-V curve was shifting toward curve (b) and the voltage was decreasing along the R_1 load line. This voltage change is seen to be caused primarily by current degradation. It can thus be inferred that this degradation was less than but not significantly different from short circuit current degradation.

Following this the voltage continued to drop to 338 mv/cell at orbit 60 even though the aspect angle was beginning to improve. It then increased to 389 mv/cell at orbit 260. During this time the angle of incidence was decreasing at a rate such that variations with the cosine law were sufficient to overcome the effects of continued current degradation. Since the operation of the cells did not quite return to curve (a), it can still be inferred that operation is similar to the R_1 load — curve (a) relationship and that readings are still fairly representative of short circuit current readings. However, because of the increase in temperature (10°C for orbits between 160 and 260) as compared to the initial temperature and because of radiation degradation, both of which decrease the I-V curve voltages, operation was, in all probability, closer to the peak power point than it was initially. The degradation would thus be a little less representative of short circuit current degradation than it was initially.

After orbit 260 and until orbit 300, the voltage readings drop slightly in spite of the fact that the angle of incidence is approaching zero. This results from the fact that radiation degradation now exceeds, though very slightly, the small enhancements due to cosine law effects plus those due to the reduction in temperature. Operation is thus inferred to be practically unchanged relative to the I-V curve and therefore readings are still fairly representative of short circuit current readings.

In the final phase (behond 300 orbits) the angle of incidence increases and the temperature decreases thus returning the I-V curve toward curve (b). With operation now in the R_1 load-curve (b) relationship, the readings again become more accurately representative of true short circuit current readings.

The results in Figures 8 and 9 are consistent with the above discussion. The degradation is relatively smooth and differs little from a nominal equivalent damage curve when plotted as short circuit current degradation but it varies considerably when plotted as a peak power degradation. The former is true because readings are nominally representative of short circuit and the latter is true because power readings on the short circuit current side of the peak power point vary linearly with voltage.

10 Ohm-cm Cells, 6 Mil Shields

The initial operating voltage for these cells was 392 mv/cell — just slightly lower than that for the 1 ohm-cm cells. However, because of the higher base resistivity, operation is shifted a little toward the peak power point as compared to the 1 ohm-cm cells. As a result the load is similar to R_4 as related to curve (a) and readings portray the initial short circuit current degradation a little less accurately as the I-V curve degrades toward curve (b) during the first 60 orbits.

Because of decreased radiation damage (compared to the 1 ohm-cm cells), the increase in operating voltage after orbit 60 continued until orbit 300 where nearly normal incidence was attained. At this time the voltage was 396 mv/cell which approaches the peak power point for the degraded cells. As a result operation is similar to R_4 as compared to curve (d). The current degradation is excessive compared to short circuit current degradation because of the drop-off in going from the short circuit current side of the knee of the I-V curve toward the peak power point.

After 300 orbits the operating point slides back up the knee as the angle of incidence increases and as degradation continues because both of these effects cause the I-V curve to collapse with the current changing much more rapidly than the voltage.

The above considerations indicate that the current degradation in the early portions (for the first 60 or more orbits) and for the later portions (around 500 orbits) of the time period studied is fairly representative of short circuit current degradation but in the proximity of 300 orbits the degradation is more representative of peak power degradation. In Figure 8 it is seen that degradations early and late in the time period studied are mutually consistent but between orbits 100 and 500 the degradation is excessive, reaching a maximum at 300 orbits.

Simultaneously, Figure 9 shows the power degradation rate between 200 and 400 orbits to be fairly steady. The degradation is thus consistent with the analysis.

1 Ohm-cm Cells, 60 Mil Shields

Since these cells were initially at a voltage of 428 mv/cell, operation is typified by R_2 and curve (a). That is, the load is quite close to the peak power point. Because of the slow degradation the voltage only dropped to 411 mv/cell before increasing with decreased angle of incidence to 447 mv/cell at normal incidence. The final voltage, at orbit 540, was again reduced to 413 mv/cell. Thus operation throughout the time period was in the vicinity of the peak power point and current variations are generally significantly different from short circuit current variations which are approached only at the lowest voltages — around orbits 60 and 540. On the other hand, with operation near the peak power point where power does not change significantly with voltage, the readings are fairly valid when used in terms of power. This is readily observed in Figures 8 and 9.

10 Ohm-cm Cells, 60 Mil Shields

Operation of this cell string was very similar to the 1 ohm-cm cell string with 60 mil shields and the above discussion applies here also.

Constant Voltage Operation

In addition to the study of the results in terms of short circuit current and peak power degradation, it is possible, because of the variations encountered, to study the current degradation at constant voltage. This parameter is important whenever a shunt regulated solar array is employed.

The 1 ohm-cm cells with 6 mil shields started operating at a voltage of 399 mv/cell. Operation never returned to this voltage but the nearest approach occurred at the 260th orbit when the voltage was 389 mv/cell. At this time the current, and hence the power (to within 3%), had degraded 28%. The 10 ohm-cm cells with the same glass returned to their initial voltage of 392 mv/cell at orbit 219 when the degradation was 23% and again at orbit 340 when the degradation was 26%. Thus, at a constant voltage of approximately 400 mv/cell, the 10 ohm-cm cells degraded less in 340 orbits than the 1 ohm-cm cells in 260 orbits — a time factor of more than 1.3.

Similarly, the 1 ohm-cm cells with 60 mil shields started at 428 mv/cell and returned to this voltage at orbit 140 and orbit 440 with degradations of 11%

and 16% respectively. The 10 ohm-cm cells with the same glass started at 419 mv/cell and returned to this voltage at orbit 100 and orbit 500 with degradations of 4% and 11% respectively. Thus, for operation near 425 mv/cell, the 1 ohm-cm cells degraded 11% in 140 orbits and the 10 ohm-cm cells degraded this same amount in 540 orbits — a time factor of 3.86.

Selected Orbits

Degradation results for selected orbits are given in Table III for general comparison purposes. The orbits were selected as follows:

a. Orbits 1-40 because aspect angle and temperature are constant.

b. Orbit 100 because voltages for the 6 mil glass strings had returned approximately to the 40 orbit value and those for the 60 mil strings had returned approximately to the initial value.

c. Orbit 300 because normal incidence is approached and the voltages are near the maximum experienced.

d. Orbit 500 because voltages had returned to a low value and were similar to those experienced in one or another of the previously selected orbits.

e. Orbit 180 because the angle of incidence was the same as in orbit 500.

Table III

DEGRADATION RESULTS FOR SELECTED ORBITS

				6 Mil Glass			60 Mil Glass		
Orbit No.	Aspect Angle (deg)	Temperature (°C)	Base Resistivity (ohm-cm)	Cell Voltage (mv)	Current Degradation (%)	Power Degradation (%)	Cell Voltage (mv)	Current Degradation (%)	Power Degradation (%)
1-40	46.7 (const)	9.8 (const)	1	399-345	13.6	25.3	428-413	3.6	7.0
			10	392-354	10.1	18.6	419-408	2.9	5.4
100	50.1	12.5	1	348	17.6	28.1	419	6.6	8.6
			10	359	13.7	20.8	419	4.1	4.1
180	63.2	19.2	1	377	23.5	27.7	437	13.7	11.9
			10	385	20.1	21.3	439	10.7	6.4
300	88.2	17.0	1	387	29.2	31.3	446	18.1	14.7
			10	396	25.6	24.6	449	14.1	8.0
500	116.8	13.5	1	321	32.9	46.0	418	14.4	16.4
			10	356	22.9	29.8	423	9.6	8.8

In addition to providing a ready comparison of degradation data, this Table also points up the significant factors in the preceding discussion.

Correlation With Laboratory Measurements

Correlation of the flight data with laboratory measurements is incomplete at this time. The primary reason for this is that space radiation spectra obtained for this orbit consisted of a detailed breakdown of the electron spectrum and a two-part breakdown of the proton spectrum. This turned out to be inadequate when it was found that as much as 99% of the damage to the cells with 6 mil shields and as much as 60% of the damage to cells with 60 mil shields was the result of proton bombardment. It appears possible to obtain the proton spectrum in sufficient detail to afford a correlation of the data, however, it is not readily available because of complications arising from the ellipticity of the orbit. It is hoped that this data will be available for inclusion in a final report at a later date. The above information is presented to indicate the importance of proton damage and the need for emphasis by design engineers for proton spectrum considerations equal to those given (because of Starfish) to the electron spectrum.

Equivalent Flux

Nominal 1 ohm-cm, bare cell equivalent flux values obtained from Figures 8 and 9 are given in Table IV. In determining these values a nominal flux was obtained for those data in Figure 8 where the current was considered representative of short circuit current and another nominal flux was obtained for those data

Table IV

Nominal Equivalent Flux Values for the Various Cell Conditions

Nominal Base Resistivity (ohm-cm)	Shield Thickness (mils)	Equivalent Flux (e/cm^2/orbit)		Flux Ratio	
		Based on Current	Based on Power	Based on Current	Based on Power
1	6	1×10^{13}	6×10^{12}	2.5	2
10	6	4×10^{12}	3×10^{12}		
1	60	1×10^{12}	6×10^{11}	4	5
10	60	5×10^{11}	2×10^{11}	2	3

in Figure 9 which are considered most representative of peak power data. These are presented in separate columns and differences in the equivalent flux, ranging from a factor of 1.3 for the 10 ohm-cm cells with 6 mil shields to 2.5 for the 10 ohm-cm cells with 60 mil shields, are readily apparent. This appears excessive at first. After considering the fact that a factor of 2 in flux represents a difference of only 5% in degradation at the end of the time period studied and after considering the generalities required in arriving at a nominal equivalent flux, the disparity loses significance. It is believed that the primary reason for the values based on power being consistently less than the values based on current is that the orbit 1 power value was low because initial operation was at a voltage below the peak power voltage in every case. Thus, the initial power was lower than the peak value and degradation when peak power is read will also be low.

In spite of the problems in the analysis of the data, the relative effectiveness of base resistivity and coverglass thickness remains clear. That is, the change in base resistivity from 1 ohm-cm to 10 ohm-cm provided a factor of 2 to 3 in radiation resistance whether 6 mil or 60 mil coverglasses were used and the change from 6 mil to 60 mil coverglass thickness provided a factor of 8 to 15 in radiation resistance whether 1 ohm-cm or 10 ohm-cm cells were used. It is evident that the use of higher base resistivity affords a significant fraction of the protection obtained with the heavy coverglass.

CONCLUSIONS AND RECOMMENDATIONS

The preliminary results of the Explorer XXVI solar cell experiment lead to the following conclusions and recommendations:

1. In orbital flight and under a wide variety of operating conditions, 10 ohm-cm N/P solar cells show significantly better radiation resistance than 1 ohm-cm N/P solar cells. The generalization of laboratory results which showed the same relationships for monoenergetic radiation was confirmed.

2. In this orbit the relative merits of the 10 ohm-cm cells and the 1 ohm-cm cells remained the same whether 6 mil or 60 mil shields were used. That is, energy dependent differences in relative radiation damage were not distinguishable.

3. The use of 10 ohm-cm cells compared to 1 ohm-cm cells provides an improvement in radiation resistance which is a significant fraction of the improvement obtained by using a 60 mil shield as compared to a 6 mil shield. It is therefore recommended that the use of higher base resistivity cells be given increased consideration by solar power system design engineers.

4. Attempts to quantitatively correlate orbital and laboratory measurements were unsuccessful because insufficient emphasis had been placed on the proton spectrum. The spectrum can be obtained and is mandatory for this orbit. Because of its significance in this orbit it is recommended that solar power systems design engineers give the proton spectrum emphasis equal to that given the electron spectrum for all orbits.

ACKNOWLEDGMENTS

The authors wish to acknowledge the fact that this work was the result of a cooperative effort by the entire Solar Power Sources Section at GSFC. Specifically the work of B. T. Barbour in fabricating the panels, Nicolas Mejia in the calibration, test and evaluation of the panels, Joseph Haynos in the study of materials, Ralph Sullivan in the solution of interface problems and the procurement of parts, and Brian Cunningham in providing helpful consultation is acknowledged. In addition, extensive assistance in the reduction of data provided by many persons under the direction of the Data Systems Division, GSFC is most gratefully acknowledged.

REFERENCES

1. R. L. Statler, "Electron-Bombardment Damage in Silicon Solar Cells", NRL Report 6091, October 1964.

2. W. R. Cherry and L. W. Slifer, "Solar Cell Radiation Damage Studies with 1 Mev Electrons and 4.6 Mev Protons", NASA TN D-2098, February 1964.

3. B. T. Cunningham, R. L. Sharp, and L. W. Slifer, "The Electrical Characteristics of Irradiated Silicon Solar Cells as a Function of Temperature", Proceedings of the Fourth Photovoltaic Specialists Conference, June 1964.

4. J. Mandelkorn et al., "Behavior of Modified Radiation-Resistant Solar Cells", Proceedings of the 15th Annual Power Sources Conference, May 1961.

5. J. G. Haynos, "Investigation of Resinous Materials for Use as Solar Cell Cover Glass Adhesives", GSFC Report X-716-65-369, September 1965.

6. R. E. Fischell, "Solar Cell Experiments on the Transit and TRAAC Satellites", Proceedings of the Solar Working Group Conference, February 1962.

7. H. Meyerson, "Some Preliminary Engineering Data From the Explorer XXVI (EPE-D) Satellite", Project Office Memorandum to Experimenters, 30 July 1965.

8. F. M. Smits, W. Rosenzweig, and W. L. Brown, "Report of Solar Cell Work at Bell Telephone Laboratories", Proceedings of the Solar Working Group Conference, February 1962.

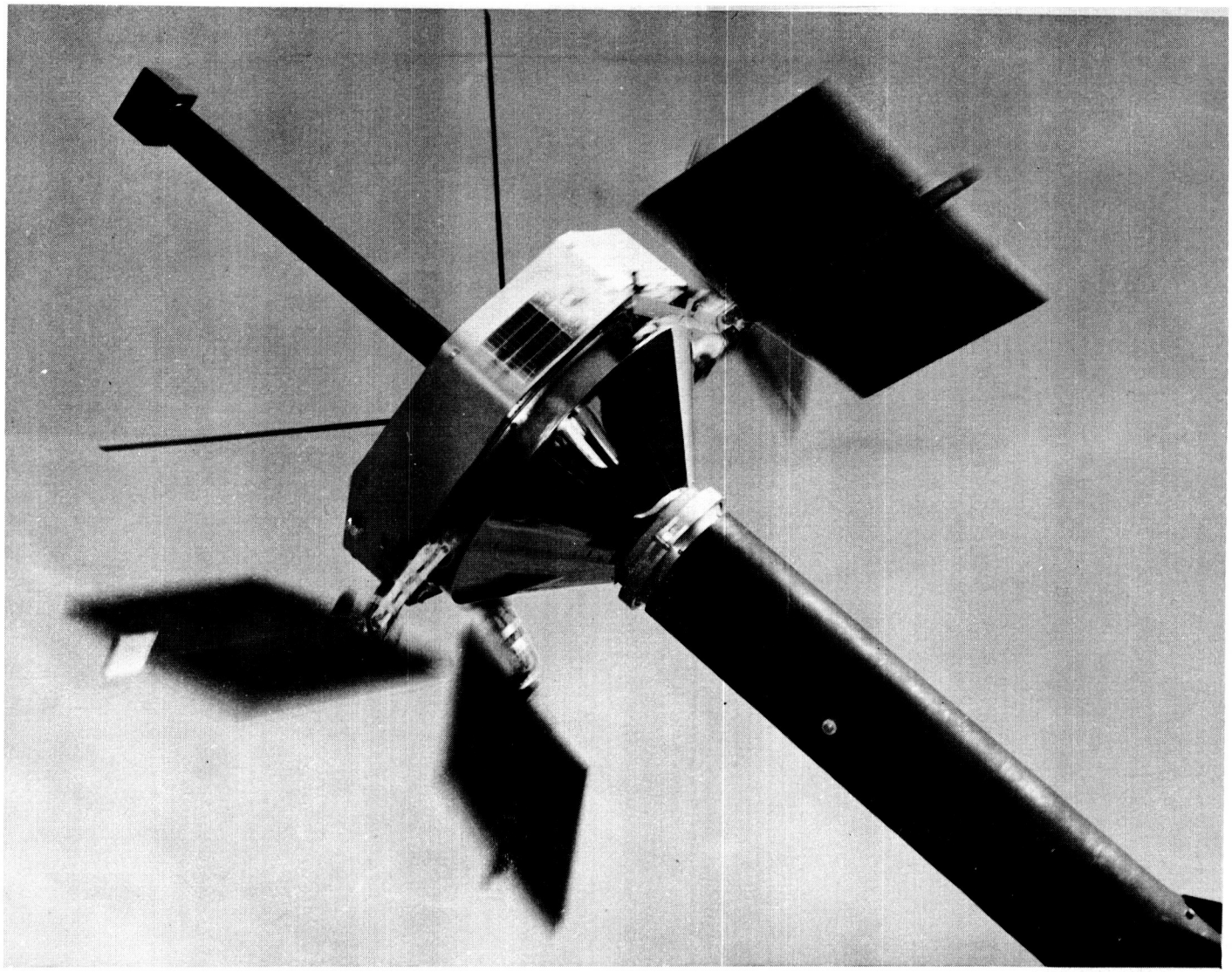

Figure 1–The Explorer XXVI Satellite During Spin Tests

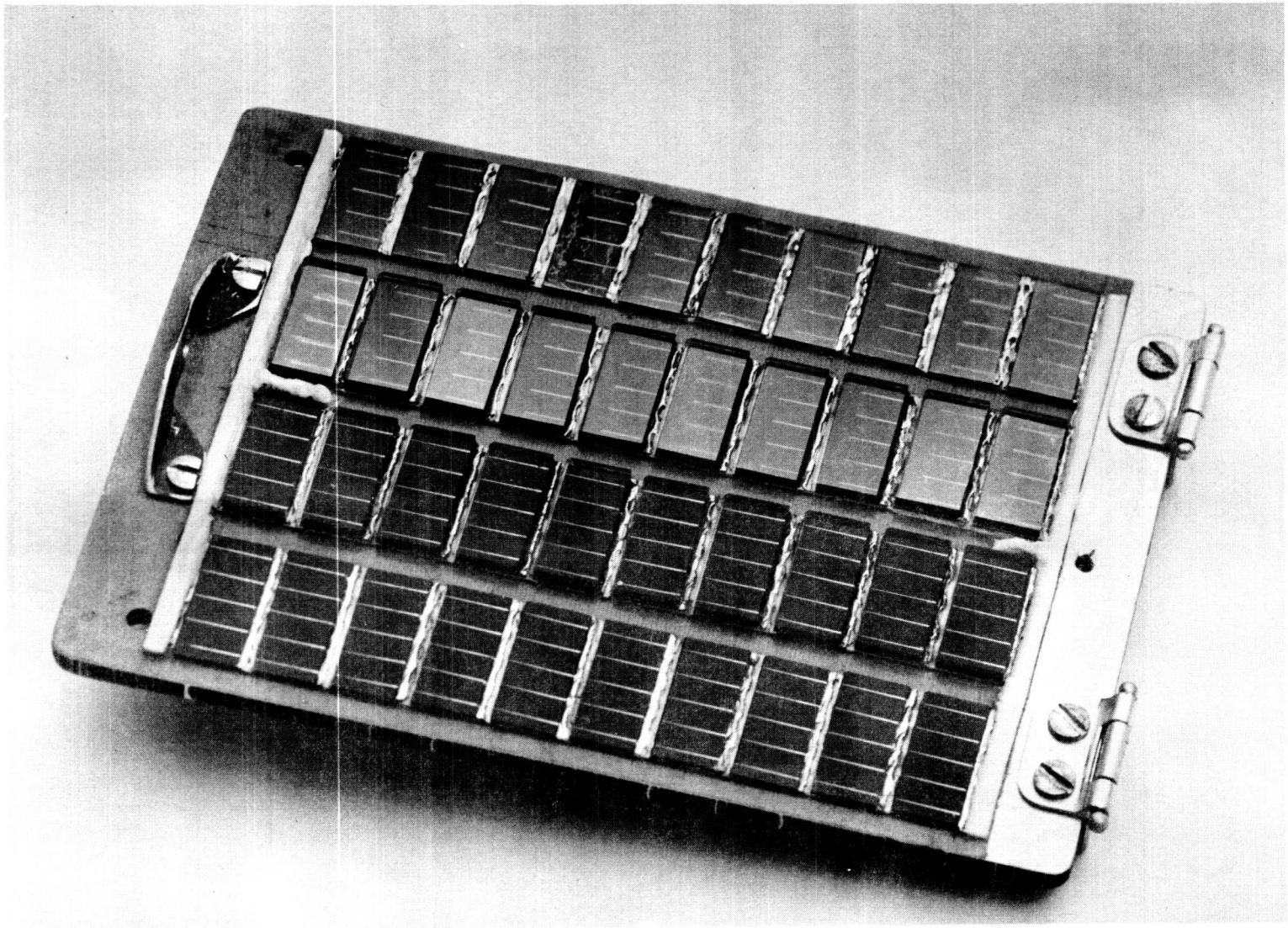

Figure 2–The Explorer XXVI Solar Cell Experiment Panel

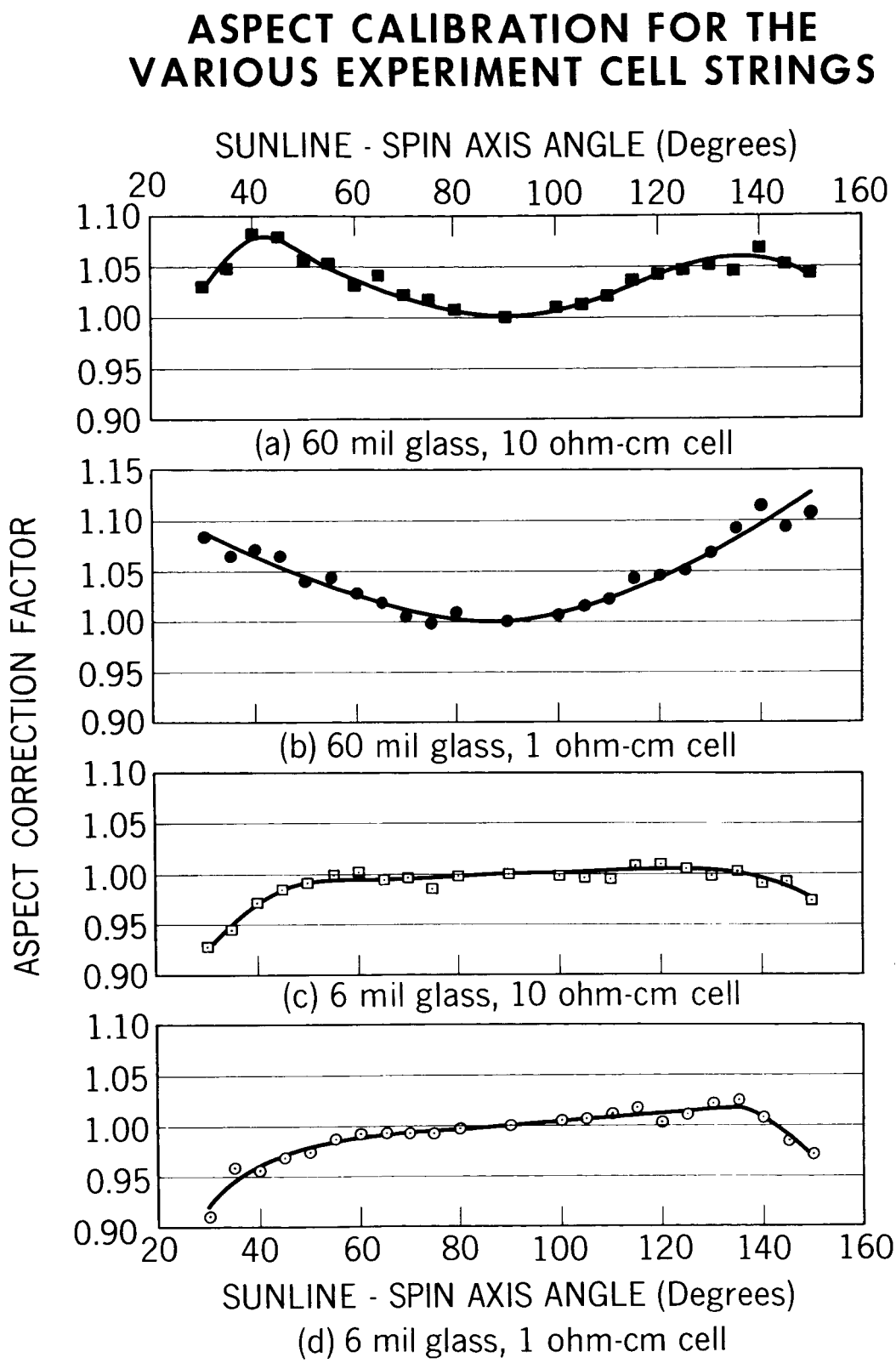

Figure 3–Aspect Calibration for the Various Experiment Cell Strings

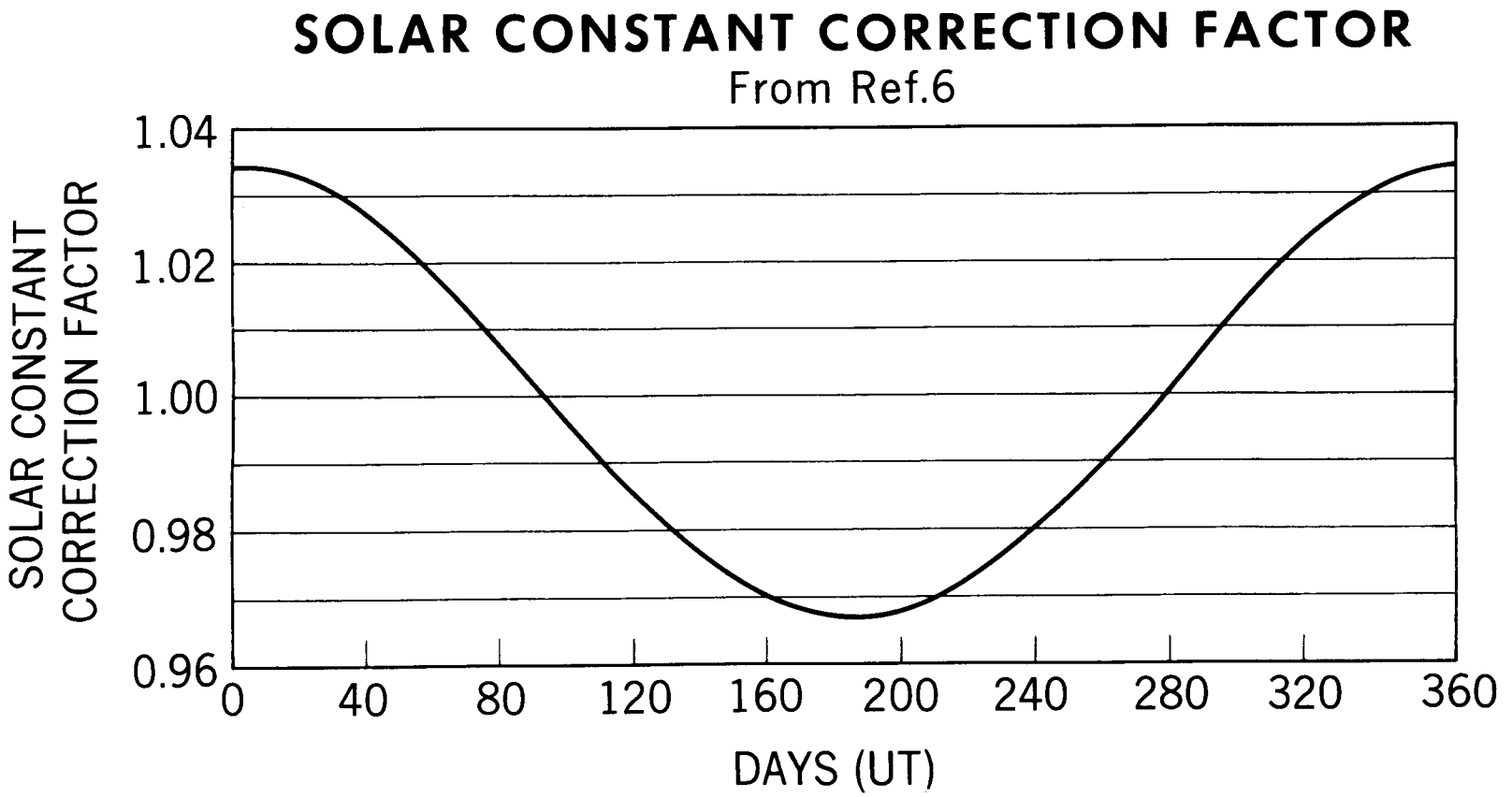

Figure 4–Solar Constant Correction Factor

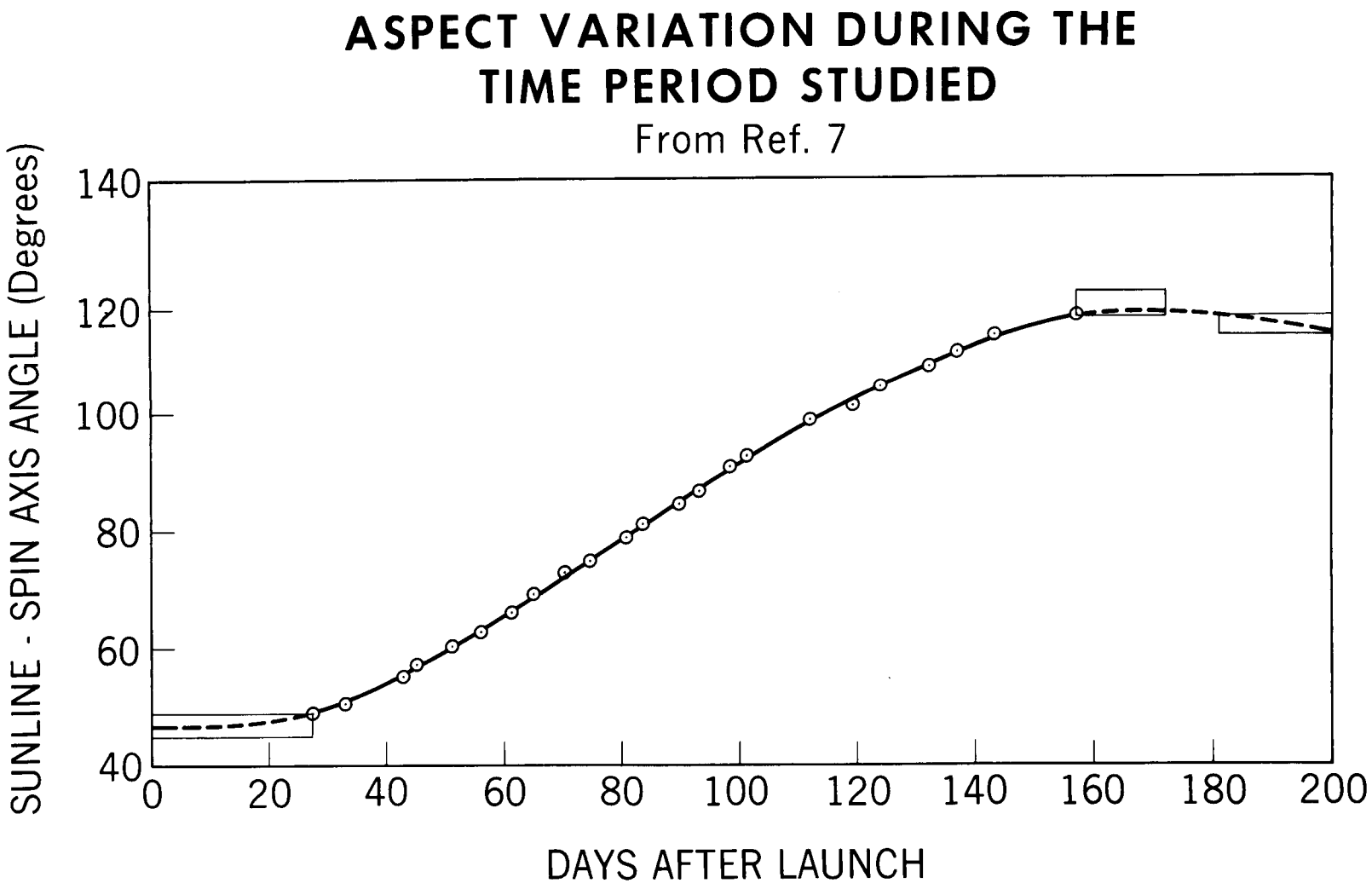

Figure 5–Aspect Variation During the Time Period Studied

EXPERIMENT PANEL TEMPERATURE VARIATION DURING THE TIME PERIOD STUDIED

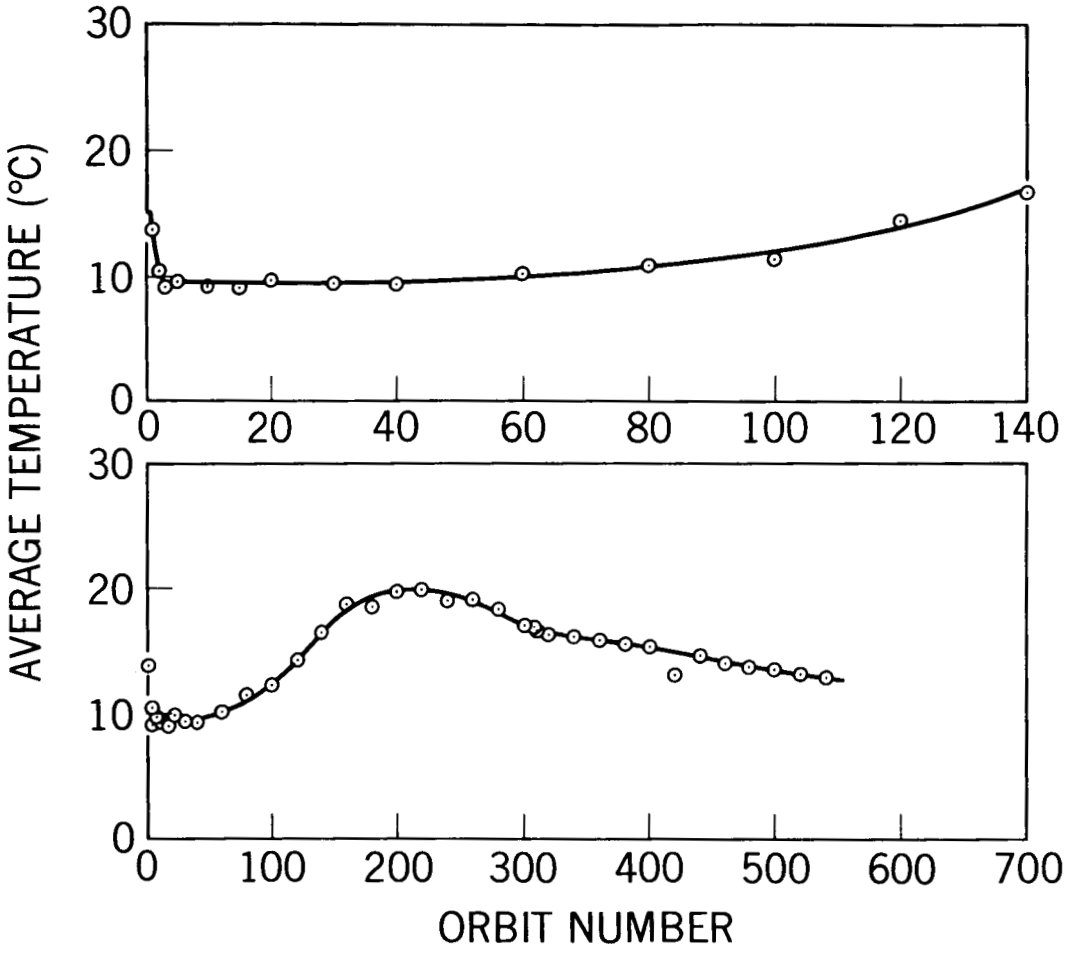

Figure 6–Experiment Panel Temperature Variation During the Time Period Studied

SOLAR CELL VOLTAGE VARIATION DURING THE TIME PERIOD STUDIED

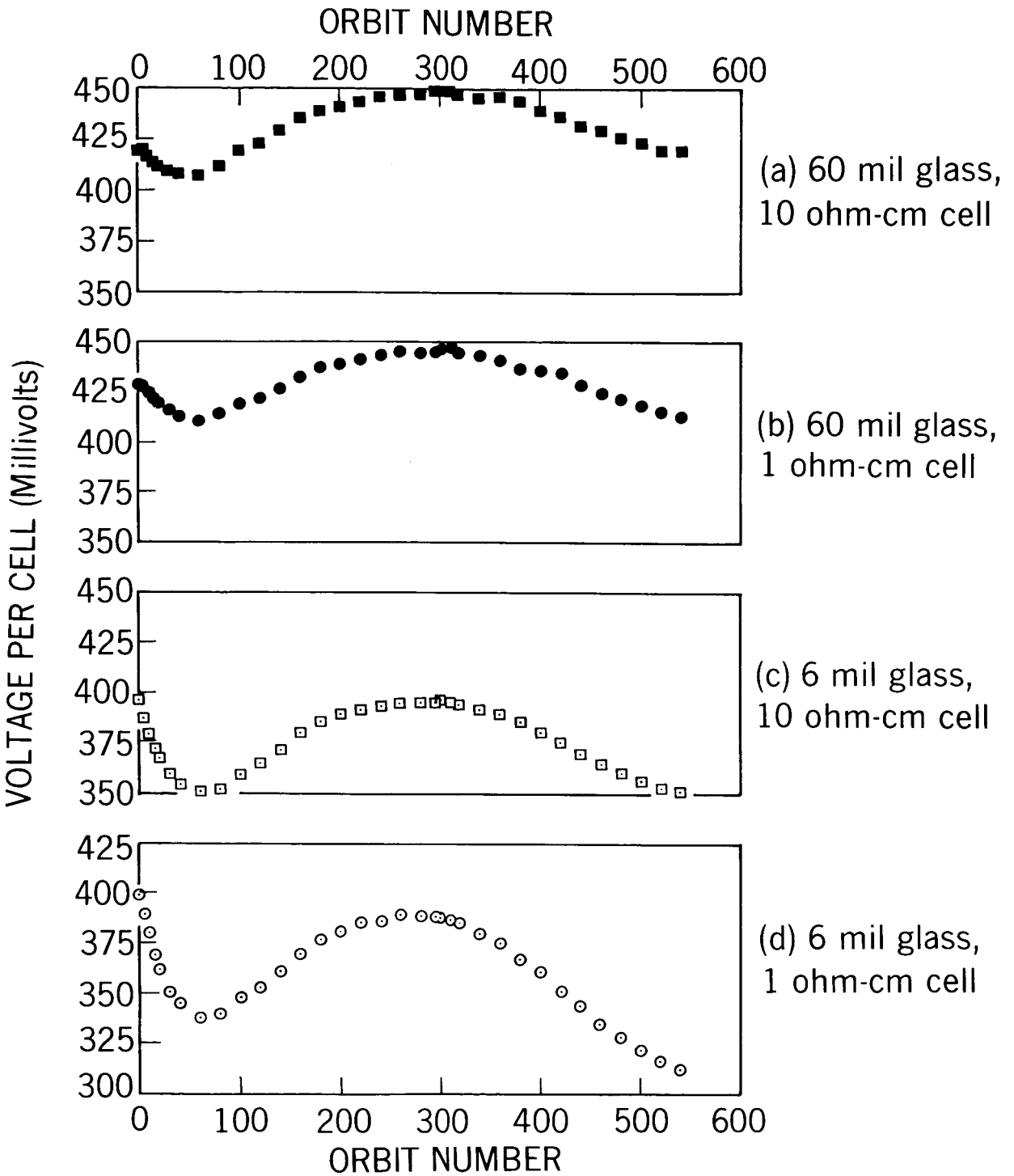

Figure 7–Solar Cell Voltage Variation During the Time Period Studied

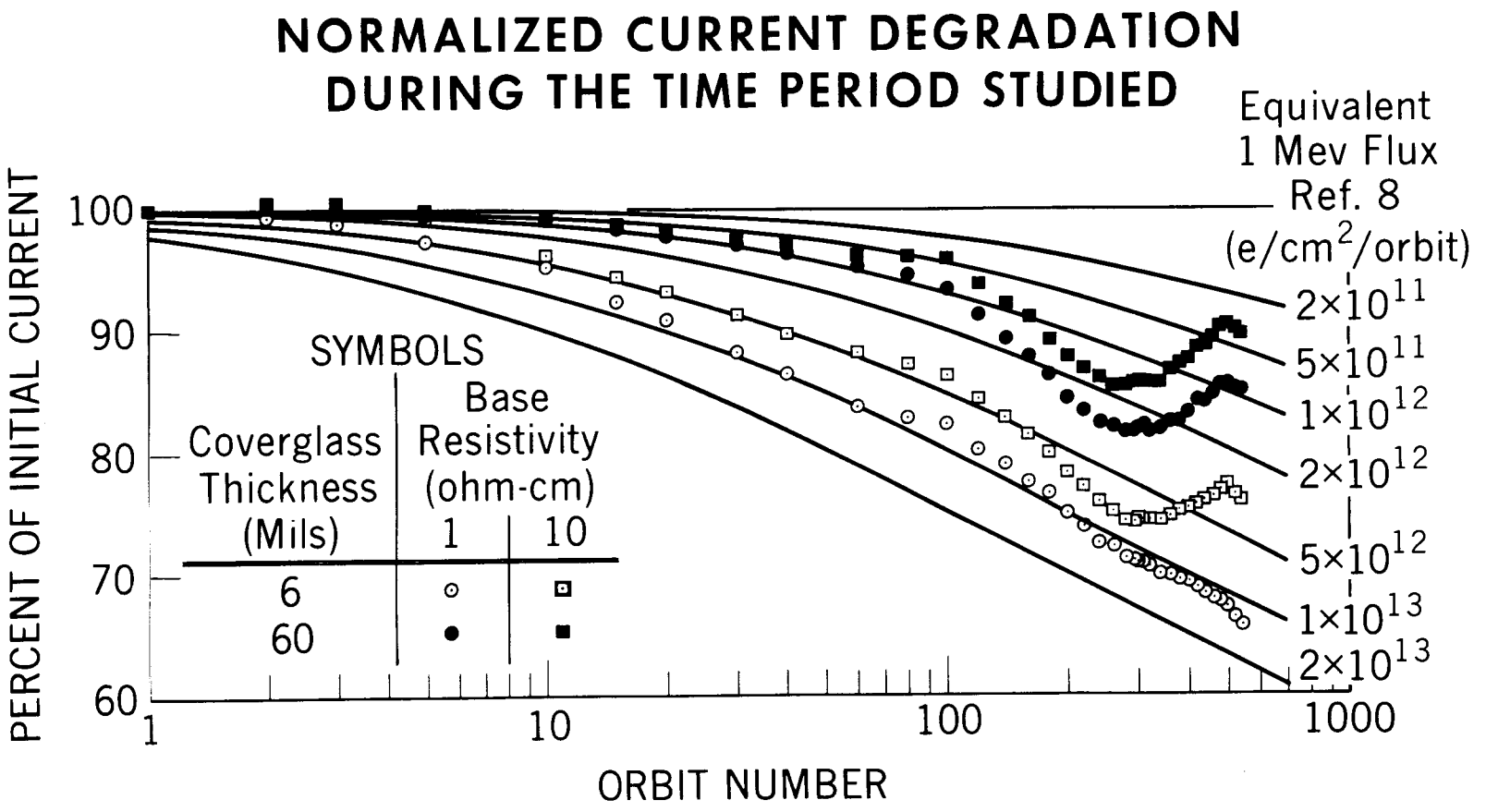

Figure 8–Normalized Current Degradation During the Time Period Studied

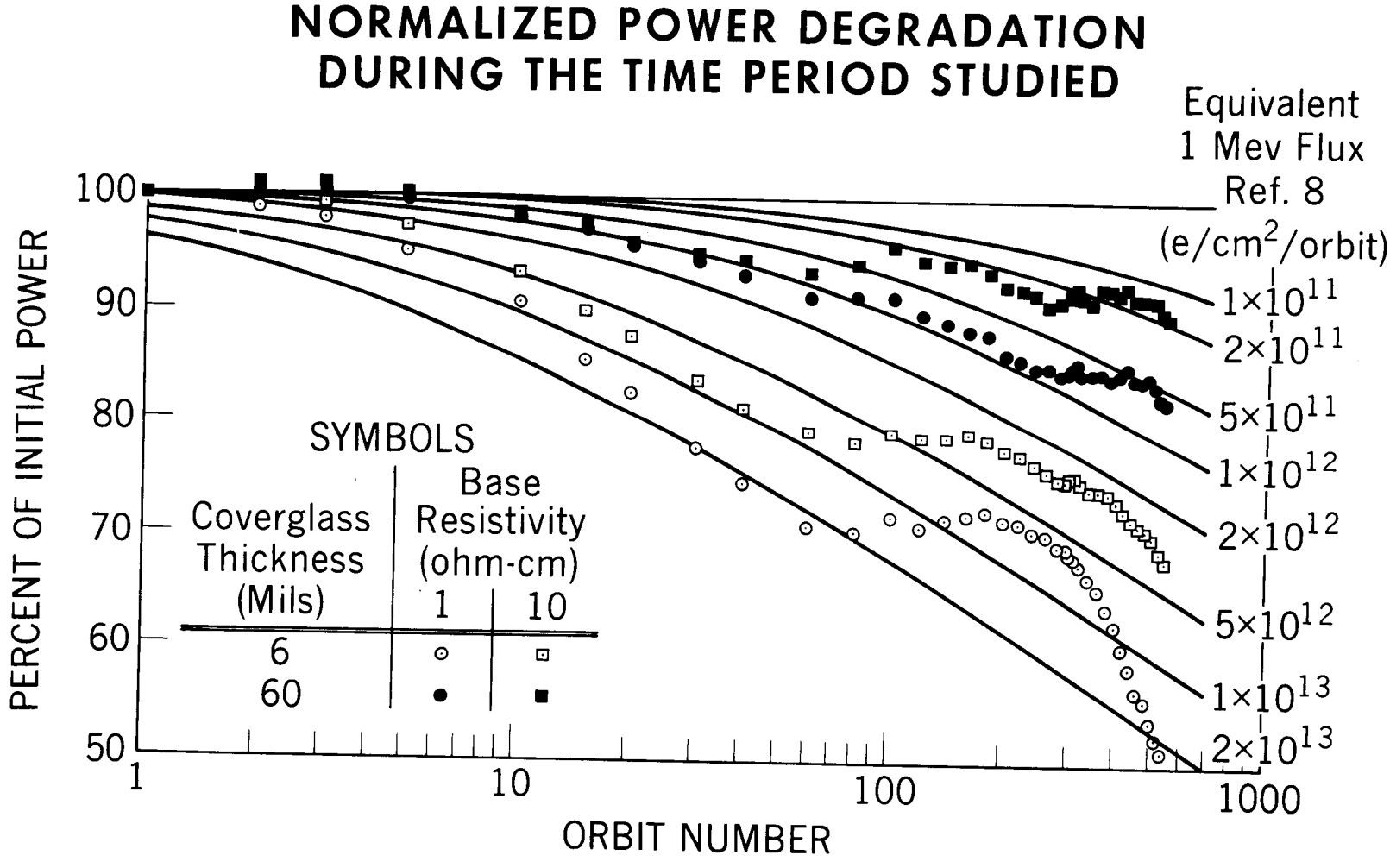

Figure 9–Normalized Power Degradation During the Time Period Studied

SKETCH DEPICTING THE EFFECT OF THE LOAD POINT ON THE DEGRADATION READINGS

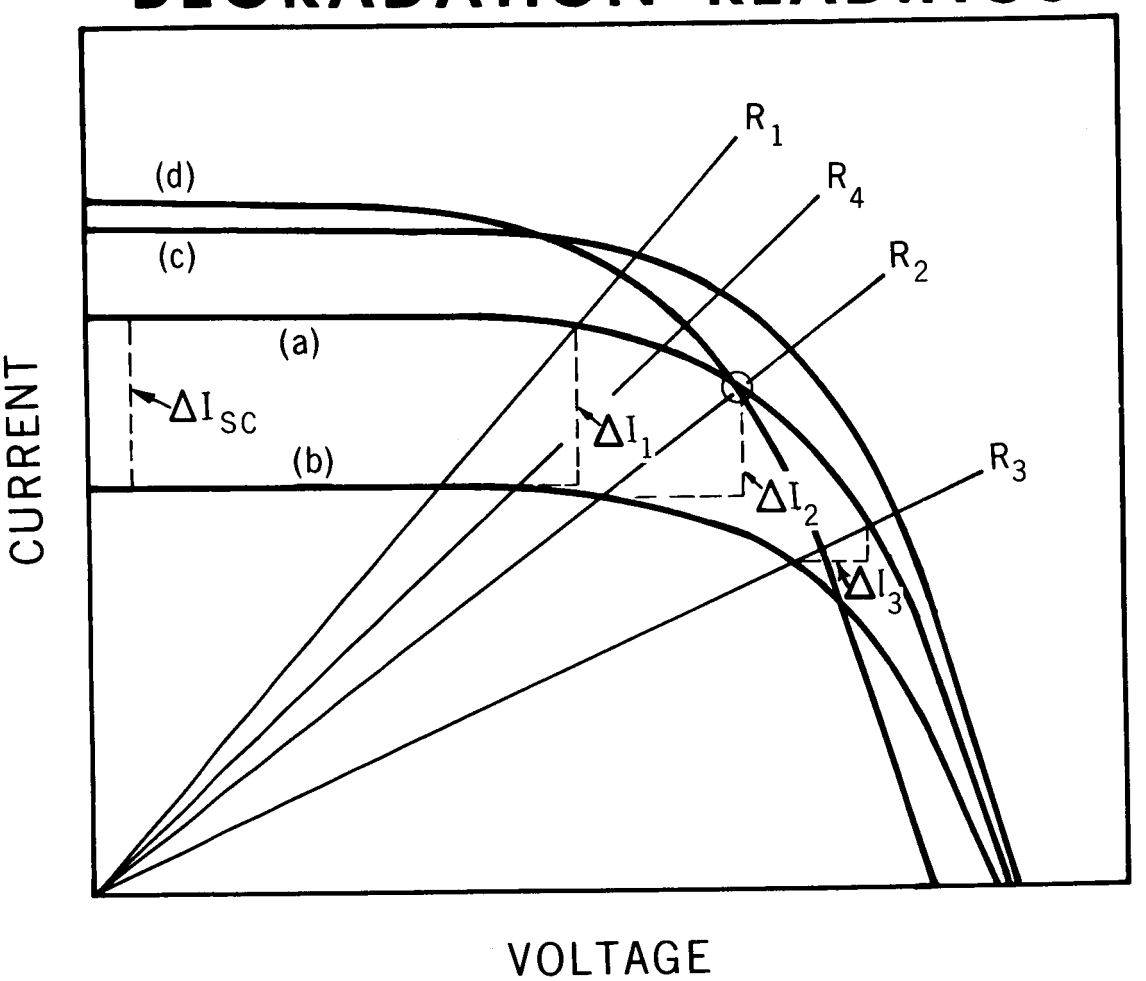

Figure 10–Sketch Depicting the Effect of the Load Point on the Degradation Readings